Evolutionary Approaches for Automatic 3D Modeling of Skulls in Forensic Identification*

J. Santamaría[1], O. Cordón[2,3], and S. Damas[2,4]

[1] Dept. Software Engineering, University of Cádiz, Cádiz, Spain
jsantam@uca.es
[2] European Centre for Soft Computing, Edf. Científico Tecnológico, Mieres, Spain
[3] Dept. of Computer Science and A.I., University of Granada, Granada, Spain
oscar.cordon@softcomputing.es, ocordon@decsai.ugr.es
[4] Dept. of Software Engineering, University of Granada, Granada, Spain
sergio.damas@softcomputing.es, sdamas@ugr.es

Abstract. Photographic supra-projection is a complex and uncertain process that aims at identifying a person by overlaying a photograph and a model of the skull found. The more accurate the skull model is the more reliable the identification decision will be. Usually, forensics are obliged to perform a manual and time consuming process in order to obtain the model of the scanned forensic object. At least semiautomatic methods are demanded by these experts to assist them with this task. Our contribution aims to propose an evolutionary-based image registration methodology for the skull 3D model building problem. Experiments are performed over thirty two problem instances corresponding to a semi-automatic and fully automatic real skull model reconstruction.

1 Introduction

Photographic supra-projection [1] is a forensic process where photographs or video shots of the missing person are compared with the skull that is found. By projecting both photographs on top of each other (or, even better, matching a scanned three-dimensional skull model against the face photo/video shot), the expert can try to establish whether that is the same person. In this paper we will focus our attention on the first stage of the process: the accurate construction of a virtual model of the skull. Specifically, our concern is its frontal part to be able to perform the craniofacial identification. Our main goal will be to provide forensics with an automatic and accurate alignment methodology.

There is a need to use a range scanner to develop a computerized study of the skull. Multiple scans from different views are required to supply the information needed to construct the 3D model. The more accurate the alignment of the views (range images) the better the reconstruction of the object. Therefore, it is

* This work is supported by the Ministerio de Educación y Ciencia (ref. TIN2006-00829), including EDRF fundings.

M. Giacobini et al. (Eds.): EvoWorkshops 2007, LNCS 4448, pp. 415–422, 2007.

fundamental to adopt a proper and robust technique to align the views in a common coordinate frame by means of *range image registration* (RIR) techniques, to avoid model distortion in the subsequent surface reconstruction stage [2].

The 3D skull model building problem when no positioning device is available is so complicated that it is one of the most time consuming tasks for the forensic experts. Therefore, software tools for the automation of their work are a real need. We will address the problem by means of a generic methodology based on *evolutionary algorithms* (EAs) for both the automatic and semiautomatic pair-wise RIR pre-alignment of several range images acquired from skulls. This proposal extends our previous contribution [3], where a *Scatter Search* (SS) EA [4] for RIR was introduced and applied to the current task. In this case, we propose a generic methodology making possible a fully automatic or at least semiautomatic approach, to help forensic experts in the first step towards the identification of a missing person. To do so, we will consider our proposal as well as other two recent EAs [5,6] within it.

The paper structure is as follows. In Section 2 we introduce the basis of our evolutionary-based methodology for the semiautomatic and fully automatic skull 3D model building. This section also presents the different evolutionary RIR techniques considered. Their suitability to tackle pair-wise RIR for 3D forensic model reconstruction is tested in Section 3 over different scenarios of skull modeling. Finally, in Section 4 we present some conclusions and future works.

2 Semiautomatic vs. Automatic Approaches for 3D Skull Model Reconstruction in Forensic Identification

Usually, pair-wise RIR methods are variants of the commonly known *Iterative Closest Point* (ICP) algorithm [7]. Since this algorithm requires a very small misalignment between the views, which is not always the case, most of the pair-wise RIR methods operate as follows [3,8]. First, a *pre-alignment* transformation or coarse alignment (a good approximation of the real one) is searched for typically by using an IR algorithm as a global search method. Then, a final *refinement* is applied, now as a local search process, typically an ICP-based method.

Depending on the range scanner precision, every view usually comprises thousands of 3D points. Since these views will be the input to our RIR problem, its complexity will depend on their sizes. If we are able to (semi)automatically synthesize these sets of points into a reduced version of them, we would both simplify the forensic expert task as well as reduce the problem complexity. To do so, we propose two different choices, according to a semiautomatic or a fully automatic RIR approach, respectively. On the one hand,*crest line extraction* [9]: where the point selection is based on the curvature of the 3D surfaces we aim at registering. On the other hand, *random sampling*, i.e., the uniform random selection of points along every 3D surface of every view.

Crest line extraction is not a trivial task. It requires the expertise of the user (in our case, the forensic expert, who has no knowledge in computer vision)

to perform a fine tuning of parameters to select only the more suitable points. However, more accurate results are expected with it, so our final aim is to be able to automatically generate a 3D skull model of enough quality without requiring the forensic expert to extract the crest lines (fully automatic approach).

There have been many proposals of pre-alignment methods that can provide a good starting point without requiring an initial guess [8]. To achieve the latter aim, our methodology will study the robustness of several evolutionary pre-alignment RIR contributions by evaluating the quality of their outcomes as proper initial estimations for the subsequent refinement step in our complex forensic anthropology scenario. For the semiautomatic approach, we have performed a crest lines extraction process by means of the Yoshizawa et al.'s proposal [9], and the points composing them are the only ones considered for the pre-alignment of the views. Then, the refinement step is applied to the original images. Any of the ICP proposals in the literature can be considered. After a preliminary experimentation, we selected Zhang's ICP-based proposal [7].

Three of the most accurate and recent evolutionary proposals in pair-wise RIR will be used used within our methodology. The reader is referred to the original contributions for more information:

- **Lomonosov et al.'s proposal:** it is focused on the use of a integer-coded *genetic algorithm* (GA) for the RIR pre-alignment problem [6].
- **Chow et al.'s proposal:** the use of a real-coded GA with suitable components is considered, like a sophisticated restart mechanism [5].
- **Santamaria et al.'s proposal:** our approach [3] is based on the adaptation of our previous IR proposal for medical MRIs [10] to apply SS to RIR.

3 Experimental Study

In this section we aim to analyze automatic and semiautomatic evolutionary approaches to generate 3D skull models of forensic objects. We will tackle the different problems the forensic expert has to deal with during the reconstruction stage of the photographic supra-projection process. Next, Section 3.1 describes the considered dataset. Sections 3.2 and 3.3 detail the experimental design and the parameter settings. Finally, Section 3.4 is devoted to the analysis of results.

3.1 Input Range Images

The Physical Anthropology Lab of the University of Granada provided us with a dataset of human skulls acquired by a Konica-Minolta© 3D Lasserscanner VI-910. We focused our study on the range images of a person who donated his remains for scientific proposes.

We have taken into account important factors along the scanning process like time and storage demand. Following the suggestions in [2], we considered a scan

every 45°. Hence, we deal with a sequence of eight different views: $0° - 45° - 90° - 135° - 180° - 225° - 270° - 315°$. The dataset we will use in our experiments is only limited to five of the eight views: $270° - 315° - 0° - 45° - 90°$. The reason is that our aim is to achieve a 3D model of the most interesting parts of the skull for the forensic expert and for the final objective of our work: the forensic identification of a missing person by photographic supra-projection.

3.2 Experimental Design

We will focus our attention on the design of pre-alignment methods as accurate, robust, and automatic as possible, especially when there is no positional device available. We will now propose a set of RIR problem instances with this aim. They will simulate an unsupervised scanning process, i.e. not oriented by any device. Likewise, we will be able to evaluate the performance of every semiautomatic and fully automatic RIR method considered as a pre-alignment technique.

For the semiautomatic approach, Yoshizawa et al.'s proposal [9] was considered to extract the crest lines. The original $270° - 315° - 0° - 45° - 90°$ views comprise 109936, 76794, 68751, 91590, and 104441 points, respectively. After crest lines extraction, the reduction in size is important: 1380, 1181, 986, 1322, and 1363 points. Figure 1 shows the correspondence between crestlines and the most prominent parts of the skull in every view. In the automatic RIR approach, we have followed an uniform random sampling of the input images. Hence, the only parameter the forensic expert must consider is the density of this random sampling. We fixed a 15% of the original dataset as a suitable value for the time and accuracy tradeoff.

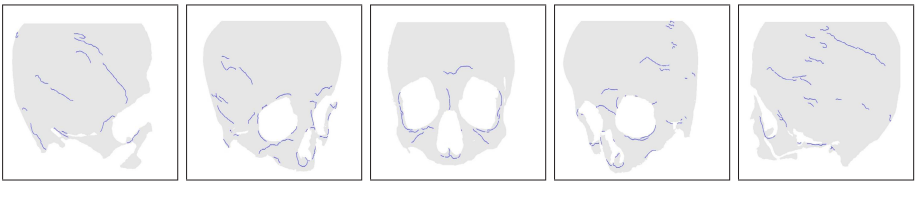

Fig. 1. From left to right: partial views of the skull and their corresponding crest lines acquired at $270°, 315°, 0°, 45°$, and $90°$, respectively

Specifically, we will consider four different rigid transformations. They are shown in Table 1 and will represent a typical bad initialization of the pre-alignment step by a forensic expert. Therefore, we are simulating the worst starting scenario. Any method that aims to become considered a good pre-alignment RIR technique will have to overcome such a bad initialization properly. These four transformations are applied to every adjacent pair of images of the 3D skull model leading to a global set of sixteen pair-wise RIR problem instances to be solved. Therefore, every method will finally deal with thirty two RIR problem instances (sixteen for every RIR approach: semi and fully automatic).

Table 1. Four rigid transformations considered

	θ	$Axis_x$	$Axis_y$	$Axis_z$	t_x	t_y	t_z
T_1	115.0°	-0.863868	0.259161	0.431934	-26.0	-15.5	-4.6
T_2	168.0°	0.676716	-0.290021	0.676716	6.0	5.5	-4.6
T_3	235.0°	-0.303046	-0.808122	0.505076	16.0	-5.5	-4.6
T_4	276.9°	-0.872872	0.436436	-0.218218	-12.0	5.5	-24.6

3.3 Parameter Settings

As we previously said, three recent contributions have been considered for our experimentation: GA_{Chow}, GA_{Lom}, and SS. Note that the first two methods perform a random sampling of several hundreds of points of the input images, in both automatic or semiautomatic approaches. Likewise, the objective function introduced in the previous proposals [5,6,3] must be slightly changed to be adapted to the strong difficulties we are imposing in this particular application, so that it considers the *Median Square Error (MedSE)* to deal with the small overlapping between adjacent views (see Figure 1):

$$MIN \quad F(f, I_s, I_m) \; = \; median\{\| \, f(\boldsymbol{p}_i) - \boldsymbol{p}_j{}' \, \|^2\}, \quad \forall \boldsymbol{p}_i \in I_s \tag{1}$$

where f is the transformation we are searching for, I_s and I_m are the input scene and model views, and $\boldsymbol{p}_j{}'$ is the closest model point to $f(\boldsymbol{p}_i)$ of the scene.

All the methods are run on a PC with an Intel Pentium IV 2.6 MHz. processor. In order to avoid execution dependence, fifteen different runs of each method in each pair-wise RIR problem instance have been performed.

We set all the parameter values in the same way that authors propose in their contributions [5,6,3]. Besides, the execution time for every pre-alignment method will be 20 and 100 seconds for the semiautomatic and fully automatic RIR approaches, respectively. The stop criterion for ICP_{Zhang} refinement stage was a maximum number of 200 iterations, which proved to be high enough to guarantee the convergence of the algorithm.

3.4 Analysis of Results

We have used the rotary stage as a positional device to actually validate the results from every RIR method. Since a high quality pre-alignment is provided from the scanner's software, a 3D model is available and it can be considered as the ground truth for the problem. Therefore, we know the global optimum location of every point in advance by using this 3D model. Unlike for the objective function, we will use the usual *Mean Square Error* (MSE) to measure the quality of the process, once the RIR method is finished. MSE is given by: $MSE = \sum_{i=1}^{r} ||f(\boldsymbol{x}_i) - \boldsymbol{x}_i{}'||^2/r$, where $f(\boldsymbol{x}_i)$ corresponds to the i-th scene point transformed by f (which is the result of every RIR method), r is the number of points in the scene image and $\boldsymbol{x}_i{}'$ is the same scene point but now using the optimal transformation f^* obtained by the positional device. Therefore, both $\boldsymbol{x}_i$

Table 2. Minimum (m), maximum (M), mean (μ), and standard deviation (σ) MSE values when tackling every problem instance (T_1, T_2, T_3, and T_4) related to the four pair-wise RIR scenarios from the **semiautomatic** approach. The best minimum (m) and mean (μ) values are highlighted using bold font

Semiautomatic RIR			T_1				T_2			
	I_{0^o} Vs. $T_i(I_{45^o})$		m	M	μ	σ	m	M	μ	σ
		SS	3.51	22.44	**11.73**	6.06	3.31	31.99	**13.54**	8.82
		$GA_{Lom.}$	1.48	5601.82	1032.79	1447.07	**1.31**	223.30	21.18	54.72
		GA_{Chow}	**1.31**	4518.76	2069.30	1858.09	1.39	4434.18	1857.96	1741.17
			T_3				T_4			
			m	M	μ	σ	m	M	μ	σ
		SS	3.41	17.30	**8.38**	5.07	3.12	13.35	**8.17**	2.69
		$GA_{Lom.}$	**1.38**	340.58	68.77	116.13	1.48	2672.86	391.27	699.74
		GA_{Chow}	2.21	5238.53	1158.02	1596.66	**1.40**	5368.14	1648.35	1526.32
	I_{0^o} Vs. $T_i(I_{315^o})$		T_1				T_2			
			m	M	μ	σ	m	M	μ	σ
		SS	**0.01**	0.01	**0.01**	0.00	**0.01**	0.01	**0.01**	0.00
		$GA_{Lom.}$	**0.01**	0.01	**0.01**	0.00	**0.01**	0.01	**0.01**	0.00
		GA_{Chow}	**0.01**	47.14	3.47	11.73	**0.01**	1084.44	79.20	269.39
			T_3				T_4			
			m	M	μ	σ	m	M	μ	σ
		SS	**0.01**	0.01	**0.01**	0.00	**0.01**	0.01	**0.01**	0.00
		$GA_{Lom.}$	**0.01**	0.03	**0.01**	0.01	**0.01**	0.01	**0.01**	0.00
		GA_{Chow}	**0.01**	43.02	4.24	11.39	**0.01**	2.07	0.16	0.51
	I_{45^o} Vs. $T_i(I_{90^o})$		T_1				T_2			
			m	M	μ	σ	m	M	μ	σ
		SS	**1.30**	1.42	**1.35**	0.04	1.32	1.41	**1.35**	0.02
		$GA_{Lom.}$	1.38	4945.76	331.77	1233.14	**1.26**	149.51	35.98	56.53
		GA_{Chow}	1.34	11348.23	801.60	2818.97	1.68	18764.62	3142.41	5722.17
			T_3				T_4			
			m	M	μ	σ	m	M	μ	σ
		SS	**1.30**	1.35	**1.32**	0.01	1.32	1.43	**1.36**	0.03
		$GA_{Lom.}$	1.39	18715.29	2513.49	6353.48	**1.26**	8708.39	582.79	2171.66
		GA_{Chow}	3.26	9569.70	805.29	2350.93	1.65	6234.63	485.92	1538.29
	I_{315^o} Vs. $T_i(I_{270^o})$		T_1				T_2			
			m	M	μ	σ	m	M	μ	σ
		SS	3.61	3.63	**3.62**	0.01	2.89	3.62	3.33	0.34
		$GA_{Lom.}$	**1.75**	11143.11	749.93	2777.70	**1.86**	4.78	**3.01**	0.78
		GA_{Chow}	2.45	5498.43	683.14	1624.90	2.34	10860.12	4238.43	5154.46
			T_3				T_4			
			m	M	μ	σ	m	M	μ	σ
		SS	2.73	3.62	**3.29**	0.36	3.62	3.62	3.62	0.00
		$GA_{Lom.}$	**1.50**	29.13	8.81	9.17	**1.73**	3.62	**2.65**	0.62
		GA_{Chow}	2.48	10777.19	2210.65	3805.84	1.87	15.55	5.62	4.25

and $\boldsymbol{x}_i{}'$ are the same point but its location can differ if $f \neq f^*$. Our aim with this MSE definition is to take advantage of the availability of an *a priori* optimum model to study the behavior of the RIR methods. Indeed, this evaluation is not applicable in real environments where no optimum model is available.

Tables 2 and 3 show the results of the semiautomatic and automatic approach, respectively. The first conclusion is the good performance of all the analyzed evolutionary proposals. Indeed, most of the minimum values (m) of all the methods in both approaches are close to zero in almost every problem instance. These results reinforce our evolutionary methodology to the pair-wise RIR in this forensic problem. On the other hand, if we compare every result in Table 2 and in Table 3 we conclude that every method behaves in a more suitable way when dealing with the semiautomatic approach than when tackling the automatic one. As it was initially expected, the synthesis of data provided by the crest lines is very helpful for every method. However, as said, this preprocessing requires the expertise for the proper crest lines extraction. Fortunately, we can see how SS is able to provide a reliable reconstruction of the skull in the automatic approach, although it is the only of the three evolutionary methods considered able to achieve this goal.

Finally, Figure 2 aims to summarize the previous comments graphically. Since we are specially interested in the automatic approach and the difference in

Table 3. Results for the **automatic** approach

Automatic RIR			T_1				T_2			
			m	M	μ	σ	m	M	μ	σ
I_{0^o} Vs. $T_i(I_{45^o})$		SS	**1.49**	11479.33	**7553.89**	2465.41	**1.37**	5630.40	**1417.78**	2351.80
		$GA_{Lom.}$	3099.70	15578.35	8401.16	4976.56	854.61	6834.97	3513.20	1649.80
		GA_{Chow}	1074.09	15143.81	8067.05	4094.66	1724.65	16093.26	5907.46	3754.55
			T_3				T_4			
			m	M	μ	σ	m	M	μ	σ
		SS	**1.50**	3112.36	**1112.95**	1399.51	**1.48**	9919.53	**6585.65**	4092.68
		$GA_{Lom.}$	4.53	3780.89	1684.41	1131.34	16.84	17851.20	7658.33	4701.49
		GA_{Chow}	208.77	10927.11	3762.57	2495.64	13.59	18101.16	9717.35	4604.05
I_{0^o} Vs. $T_i(I_{315^o})$			T_1				T_2			
			m	M	μ	σ	m	M	μ	σ
		SS	**0.01**	0.01	**0.01**	0.00	**0.01**	0.01	**0.01**	0.00
		$GA_{Lom.}$	**0.01**	82.40	8.16	21.05	**0.01**	6433.83	611.05	1689.94
		GA_{Chow}	**0.01**	7162.80	1189.77	2225.74	**0.01**	21165.96	8258.95	7664.76
			T_3				T_4			
			m	M	μ	σ	m	M	μ	σ
		SS	**0.01**	0.01	**0.01**	0.00	**0.01**	0.01	**0.01**	0.00
		$GA_{Lom.}$	**0.01**	15292.79	8034.59	6503.39	**0.01**	6429.36	1273.88	2519.95
		GA_{Chow}	**0.01**	17992.58	6658.78	7166.29	**0.01**	14673.30	1664.11	3612.26
I_{45^o} Vs. $T_i(I_{90^o})$			T_1				T_2			
			m	M	μ	σ	m	M	μ	σ
		SS	**1.24**	19518.23	7638.99	9355.58	**1.18**	18781.22	**1253.63**	4684.44
		$GA_{Lom.}$	1.78	19420.03	**6452.13**	9058.42	1.34	19601.43	5172.05	8502.45
		GA_{Chow}	2.24	19952.58	13358.92	8227.04	1.34	19816.55	7776.61	9176.55
			T_3				T_4			
			m	M	μ	σ	m	M	μ	σ
		SS	**1.13**	19400.45	**2586.27**	6590.61	**1.10**	1.27	**1.24**	0.03
		$GA_{Lom.}$	1.25	19411.10	3864.91	7705.66	1.31	18795.58	2518.45	6373.43
		GA_{Chow}	3.61	19505.41	12540.78	8854.98	2.42	19768.89	11240.35	8760.94
I_{315^o} Vs. $T_i(I_{270^o})$			T_1				T_2			
			m	M	μ	σ	m	M	μ	σ
		SS	2.72	20375.45	**1361.59**	5081.66	2.72	21605.61	5742.59	9517.60
		$GA_{Lom.}$	**2.45**	20000.45	2658.30	6767.95	2.61	20600.98	**1377.29**	5137.74
		GA_{Chow}	2.65	20192.43	13260.02	8590.65	**2.57**	20139.24	10200.25	8796.53
			T_3				T_4			
			m	M	μ	σ	m	M	μ	σ
		SS	2.81	21290.11	**2788.46**	7101.72	**2.02**	3.62	**3.20**	0.5
		$GA_{Lom.}$	**2.47**	19951.30	3951.35	7893.31	2.29	4.17	3.42	0.5
		GA_{Chow}	2.48	21362.86	9265.16	9920.66	2.60	21155.96	5491.44	9085.52

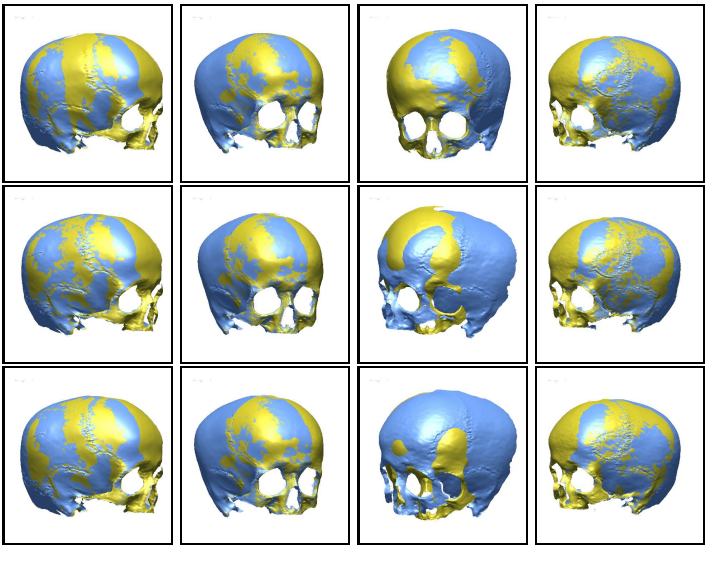

Fig. 2. From top to bottom: the worst minimum results (i.e. the worst m in every $\{T_1, T_2, T_3, T_4\}$ set) of the four pair-wise RIR scenarios corresponding to SS (first row), GA_{Lom} (second row), and GA_{Chow} (third row)

performance is more easily identified in it, we will focus on this approach. Specifically, we present the worst minimum results (i.e. the worst m in every $\{T_1, T_2, T_3, T_4\}$ set) of the four pair-wise RIR scenarios corresponding to SS (first row), GA_{Lom} (second row), and GA_{Chow} (third row). Such worst-case visualization will stress the difference in performance among the proposals of this methodology. In particular, note the difficulties when tackling the $I_{0^o}\ Vs.\ T_i(I_{45^o})$ scenario corresponding to the third column of the figure except for the SS method (first row).

4 Concluding Remarks

We have detailed the suitability of range scanners for the reconstruction of reliable models in the forensic photographic supra-projection process. There are scenarios where a positional device which automatically builds the model cannot be used. Moreover, the latter devices often fail when solving the problem. We have proposed a semiautomatic/automatic evolutionary methodology to solve the previous problems and we have analyzed three recent EAs as pair-wise RIR methods [5,6,3] within it. From the results obtained, we have demonstrated that a fully automatic approach is possible by using our SS-based proposal [3], outperforming the other two methods considered in terms of performance and robustness. We are planning to extend this study to other pre-alignment methods [8] within the proposed methodology.

References

1. M. Y. Iscan: Introduction to techniques for photographic comparison. In M. Y. Iscan and R. Helmer, Eds., Forensic Analysis of the Skull, Wiley, 57–70, 1993.
2. L. Silva, O. Bellon, and K. Boyer: Robust range image registration using genetic algorithms and the surface interpenetration measure. World Scientific, 2005.
3. J. Santamaría, O. Cordón, S. Damas, I. Alemán, and M. Botella: A Scatter Search-based technique for pair-wise 3D range image registration in forensic anthropology. Soft Computing, In press, 2007.
4. M. Laguna and R. Martí: Scatter search: methodology and implementations in C. Kluwer Academic Publishers, 2003.
5. C. K. Chow, H.T. Tsui, and T. Lee: Surface registration using a dynamic genetic algorithm. Pattern Recognition, 37: 105–117, 2004.
6. E. Lomonosov, D. Chetverikov, and A. Ekart: Pre-registration of arbitrarily oriented 3D surfaces using a GA. Pattern Rec. Letters 27(11): 1201–1208, 2006.
7. Z. Zhang: Iterative point matching for registration of free-form curves and surfaces. International Journal of Computer Vision, 13(2): 119–152, 1994.
8. J. Salvi, C. Matabosch, D. Fofi, and J. Forest: A review of recent range image registration methods with accuracy evaluation. Image Vision Comp., In press, 2007.
9. S. Yoshizawa, A. Belyaev, and H. Seidel: Fast and robust detection of crest lines on meshes. Proc. 2005 ACM Symp. on Solid and Physical Modeling, 227–232, 2005.
10. O. Cordón, S. Damas, and J. Santamaría: A fast and accurate approach for 3D image registration using the scatter search evolutionary algorithm. Pattern Recognition Letters, 27(11): 1191–1200, 2006.